

Received 31 December 2019
Accepted 2 April 2020

Edited by W. T. A. Harrison, University of Aberdeen, Scotland

Keywords: piperidin-4-one; crystal structure; Hirshfeld surface.

CCDC reference: 1994539

Supporting information: this article has supporting information at journals.iucr.org/e

Synthesis, crystal structure, DFT calculations and Hirshfeld surface analysis of 3-butyl-2,6-bis(4-fluorophenyl)piperidin-4-one

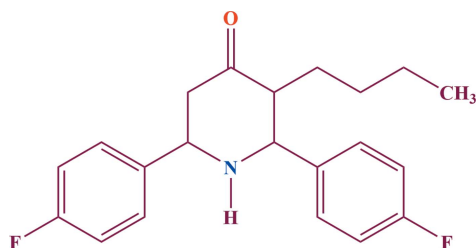
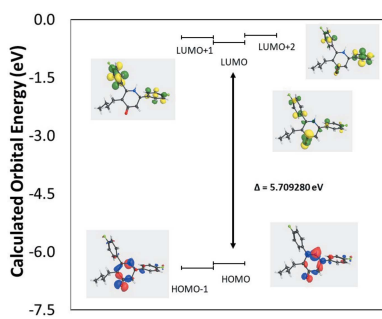
K. Anitha,^a S. Sivakumar,^{a,b*} R. Arulraj,^c K. Rajkumar,^a Manpreet Kaur^d and Jerry P. Jasinski^{d*}

^aResearch and Development Centre, Bharathiar University, Coimbatore, Tamilnadu 641 046, India, ^bDepartment of Chemistry, Thiruvalluvar Arts and Science College, Kurinjiapadi, Tamilnadu 607 302, India, ^cDepartment of Electrical and Computer Engineering, National University of Singapore, Singapore 117 583, and ^dDepartment of Chemistry, Keene State College, 229 Main Street, Keene, NH 03435-2001, USA. *Correspondence e-mail: sivakumar.phd2016@gmail.com, jjasinski@keene.edu

The title compound, C₂₁H₂₃F₂NO, consists of two fluorophenyl groups and one butyl group equatorially oriented on a piperidine ring, which adopts a chair conformation. The dihedral angle between the mean planes of the phenyl rings is 72.1 (1)°. In the crystal, N—H···O and weak C—H···F interactions, which form R₂²[14] motifs, link the molecules into infinite C(6) chains propagating along [001]. A weak C—H···π interaction is also observed. A Hirshfeld surface analysis of the crystal structure indicates that the most significant contributions to the crystal packing are from H···H (53.3%), H···C/C···H (19.1%), H···F/F···H (15.7%) and H···O/O···H (7.7%) contacts. Density functional theory geometry-optimized calculations were compared to the experimentally determined structure in the solid state and used to determine the HOMO–LUMO energy gap and compare it to the UV–vis experimental spectrum.

1. Chemical context

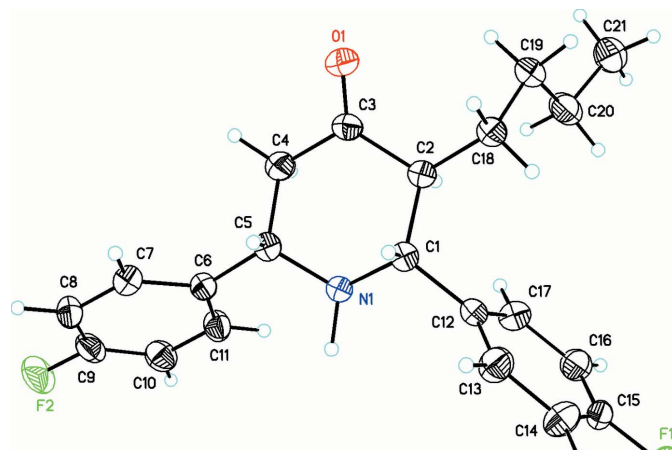
Piperidin-4-one compounds have various biological properties and have applications as anti-viral, antitumor, and anti-histaminic agents (El-Subbagh *et al.*, 2000; Mobio *et al.*, 1989; Katritzky & Fan, 1990; Arulraj *et al.*, 2020). 2,6-Disubstituted piperidine-4-ones commonly adopt a chair conformation for the heterocyclic ring (see, for example, Rajkumar *et al.*, 2018). However, on varying the substituents attached to the phenyl ring, the conformation of the ring may change (*e.g.* Ramachandran *et al.*, 2007; Arulraj *et al.*, 2020). Additionally, the attached functional group on the crystalline compound is important to determine the activity of the compound in the area of drug discovery.



As part of our studies in this area, we now describe the synthesis and structure of the title compound, C₂₁H₂₃F₂NO, (I), in order to establish the structural effects of the butyl and fluoro groups on the conformation. DFT calculations and a Hirshfeld analysis have also been carried out.



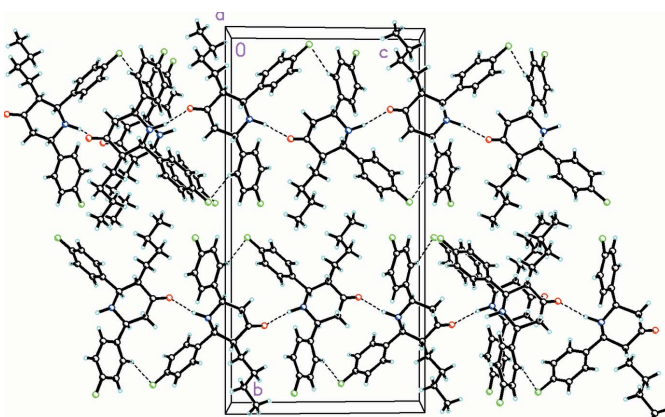
OPEN ACCESS

**Figure 1**

A view of the molecular structure of $C_{21}H_{23}F_2NO$, showing displacement ellipsoids drawn at the 30% probability level.

2. Structural commentary

Compound (I) crystallizes in space group $P2_1/c$ with one molecule in the asymmetric unit (Fig. 1). In the arbitrarily chosen asymmetric unit, the stereogenic centres have the following configurations: C1 *S*, C2 *R* and C5 *R*, but crystal symmetry generates a racemic mixture. The piperidine ring adopts a slightly distorted chair conformation with puckering parameters $Q = 0.5864$ (16) Å, $\theta = 6.56$ (15)°, $\varphi = 356.9$ (14)°. The dihedral angles for the C1–C5/N1 (all atoms) piperidine (*A*), C6–C11 fluorophenyl (*B*) and C12–C17 fluorophenyl (*C*) rings are $A/B = 65.50$ (8), $A/C = 73.87$ (8) and $B/C = 72.11$ (8)°. The substituents on the piperidine ring adopt equatorial orientations with the keto oxygen atom being anti-clinal [$O1-C3-C2-C1 = -124.44$ (16)°]. The butyl group lies in a syn-periplanar orientation [$O1-C3-C2-C18 = 0.7$ (2)] while the fluorophenyl groups are both anti-clinal [$N1-C5-C6-C7 = -148.28$ (13) and $N1-C1-C12-C17 = -75.42$ (16)°]. The sum of the bond angles around N1 is 336.8°, which is consistent with sp^3 hybridization for this atom (Beddoes *et al.*, 1986).

**Figure 2**

Crystal packing for $C_{21}H_{23}F_2NO$ viewed along the *a*-axis direction. Dashed lines indicate $N-H\cdots O$ hydrogen bonds and weak $C-H\cdots F$ interactions forming $R_2^2(14)$ loops and infinite $C(6)$ chains (*via* the $N-H\cdots O$ bond) along the *c*-axis direction.

Table 1
Hydrogen-bond geometry (Å, °).

$Cg3$ is the centroid of the C12–C17 ring.

$D-H\cdots A$	$D-H$	$H\cdots A$	$D\cdots A$	$D-H\cdots A$
$N1-H1\cdots O1^i$	1.05	2.06	3.0921 (16)	165
$C7-H7\cdots F1^{ii}$	0.95	2.52	3.3291 (18)	143
$C10-H10\cdots O1^{iii}$	0.95	2.66	3.470 (2)	144
$C16-H16\cdots F2^{iv}$	0.95	2.62	3.3680 (18)	136
$C21-H21C\cdots F2^{ii}$	0.98	2.58	3.489 (2)	154
$C21-H21A\cdots Cg3^v$	0.98	2.95	3.793 (2)	145

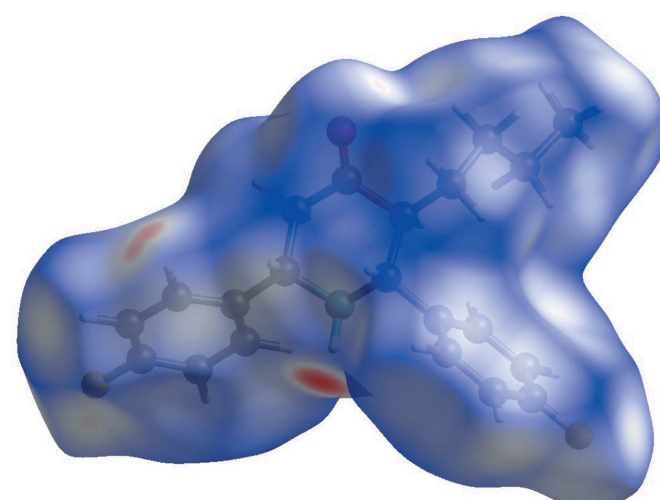
Symmetry codes: (i) $x, -y + \frac{1}{2}, z + \frac{1}{2}$; (ii) $x, -y + \frac{1}{2}, z - \frac{1}{2}$; (iii) $x - 1, -y + \frac{1}{2}, z + \frac{1}{2}$; (iv) $-x + 1, y + \frac{1}{2}, -z + \frac{3}{2}$; (v) $-x + 2, -y + 1, -z + 1$.

3. Supramolecular features

$N1-H1\cdots O1$ and weak $C7-H7\cdots F1$ interactions are observed in the crystal of (I) (Table 1, Fig. 2), which form $R_2^2(14)$ graph-set ring motifs and infinite $C(6)$ chains (*via* the $N-H\cdots O$ bond) along [001]. Some longer $C-H\cdots O$ and $C-H\cdots F$ contacts are also present as well as a single weak $C-H\cdots \pi$ interaction (Table 1).

4. Hirshfeld surface analysis

A Hirshfeld surface (HS) analysis (Spackman & Jayatilaka, 2009) was carried out using *CrystalExplorer17.5* (Turner *et al.*, 2017) to visualize the intermolecular interactions in (I). The bright-red spot near H1 indicates its role as a hydrogen-bond donor to O1 (Fig. 3) and another red region near H7 correlates with the $C7-H7\cdots F1$ interaction. The shape-index of the HS represents a way to visualize $\pi\cdots\pi$ stacking by the presence of red and/or blue triangles but there are none in the title compound (see Figure S1 in the supporting information). The curvedness of the HS can be used to divide the molecular surface into contact patches with each neighbouring molecule thereby using it to define a coordination number in the crystal (see Figure S2 in the supporting information).

**Figure 3**

A view of the three-dimensional Hirshfeld surface for $C_{21}H_{23}F_2NO$, plotted over d_{norm} in the range -0.39 to 1.31 a.u.

Two-dimensional fingerprint plots show the relative contributions of the various types of contacts to the Hirshfeld surface for (I) (McKinnon *et al.*, 2007). The overall plot is shown in Fig. 4a. The H···H contacts (53.3%) are the most important interactions (Fig. 4b), presumably because of the large hydrogen content of (I), with a pair of blue-coloured blunt spikes directing towards the bottom left, in the region $1.20 \text{ \AA} < (d_e + d_i) < 1.19 \text{ \AA}$. The pair of wings for the H···C/C···H contacts (Fig. 4c; 19.1% contribution to the HS) is in the region $1.04 \text{ \AA} < (d_e + d_i) < 1.58 \text{ \AA}$ and includes the weak C—H··· π interaction. The H···F/F···H contacts (Fig. 4d; 15.7% contribution) are seen as a pair of wings in the region $1.04 \text{ \AA} < (d_e + d_i) < 1.38 \text{ \AA}$. The wings for the H···O/O···H contacts (Fig. 4e; 7.7% contribution) are in the region of $0.88 \text{ \AA} < (d_e + d_i) < 1.20 \text{ \AA}$ while the blunt wings in the plot

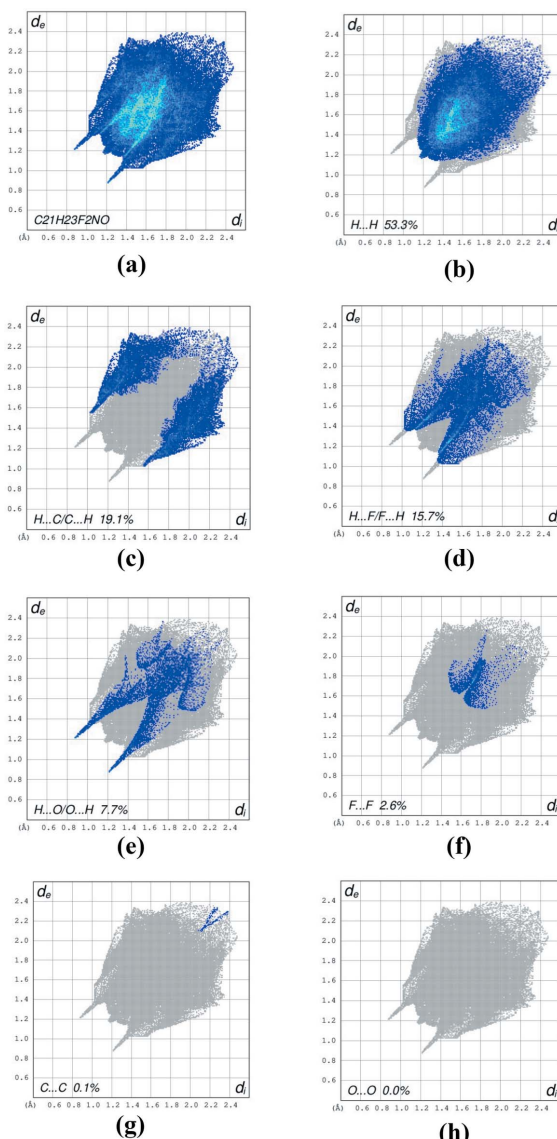


Figure 4

A view of the two-dimensional fingerprint plots for $C_{21}H_{23}F_2NO$, showing (a) all interactions, and separated into (b) H···H, (c) H···C/C···H, (d) H···F/F···H, (e) H···O/O···H, (f) F···F, (g) C···C and (h) O···O interactions. The d_i and d_e values are the closest internal and external distances (in \AA) from given points on the Hirshfeld surface contacts.

for F···F contacts (Fig. 4f; 2.6%) are in the region $1.60 \text{ \AA} < (d_e + d_i) < 1.70 \text{ \AA}$. The C···C contacts (Fig. 4g) make a negligible 0.1% contribution and are viewed as a dash pattern pointing diagonally left. The O···O contacts (Fig. 4h) make no contribution to the HS. The most significant of these contributions to the overall Hirshfeld surface are shown in Figure S3 in the supporting information.

5. DFT Calculations

A density functional theory (DFT) geometry-optimized calculation for (I) was carried out using *WebMo Pro* (Schmidt & Polik, 2007) in the *GAUSSIAN 09* program package (Frisch *et al.*, 2009) using the 6-31+G(d) basis set (Hehre *et al.*, 1986). The starting geometry was taken from the crystal structure and no solvent correction was applied. A comparison of bond angles and bond distances in the crystal to those from the DFT calculation are listed in supplementary Table S1, which generally shows good agreement. An overlay of the geometry-optimized calculation with the crystal structure has an r.m.s. deviation of 0.478 \AA . The major difference between the experimental and calculated structures occurs in the orientation of the C12–C17 rings, which are rotated by $41.8(6)^\circ$ with respect to each other.

The calculated energies (eV) for the frontier molecular orbitals are shown in Fig. 5 and key parameters are listed in supplementary Table S2. Both the HOMO and HOMO–1 are localized largely on the piperidine ring. For the LUMO, LUMO+1 and LUMO+2, the orbitals are delocalized over the piperidine ring as well as both phenyl rings. The observed UV/vis absorption spectrum (Fig. 6) shows two band envelopes with λ_{max} values located at *ca* 256 and 216 nm (~ 4.84 and 5.74 eV). The molar extinction coefficients, ε , are 1.12 and $2.50 \text{ l mol}^{-1} \text{ cm}^{-1}$, respectively. We tentatively assign the first absorption band envelope at 256 nm to overlapping contri-

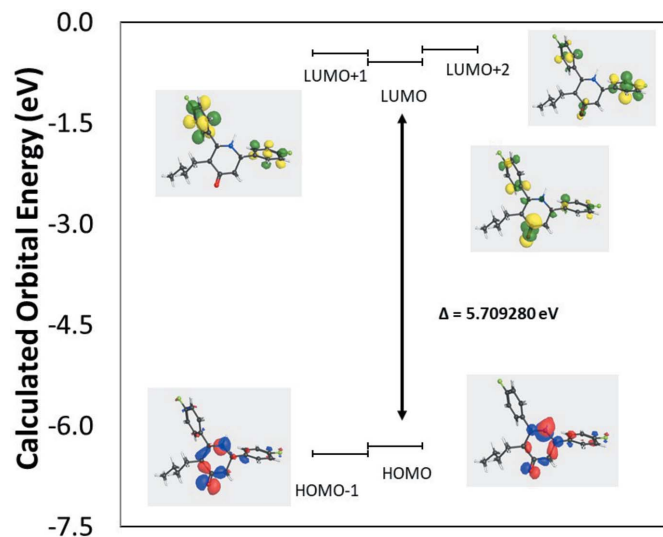


Figure 5
Schematic MO diagram.

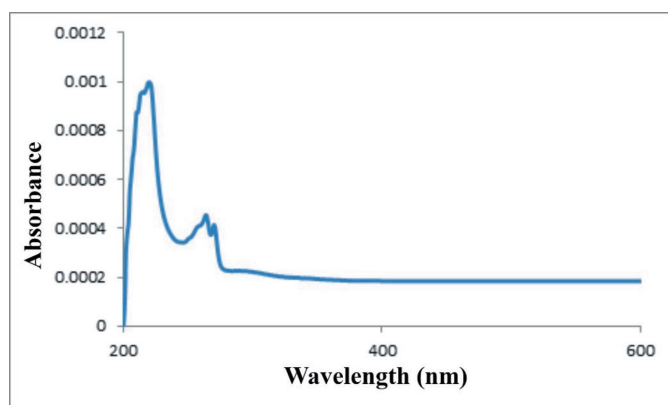


Figure 6
UV-vis spectrum of $C_{21}H_{23}F_2NO$

butions from HOMO \rightarrow LUMO (energy gap 5.71 eV), HOMO \rightarrow LUMO+1 (5.83 eV) and HOMO-1 \rightarrow LUMO (5.82 eV). The band at 216 nm is assigned to overlapping contributions from HOMO \rightarrow LUMO+2 (5.89 eV), HOMO-1 \rightarrow LUMO+1 (5.95 eV) and HOMO-1 \rightarrow LUMO+2 (6.01 eV).

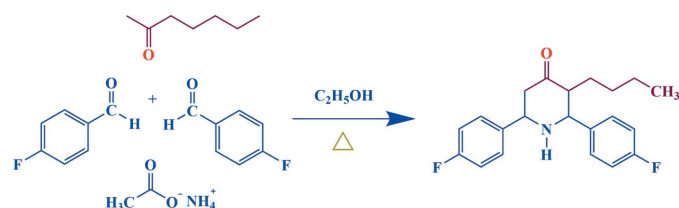
6. Database survey

A search in the Cambridge Crystallographic Database (CSD version 2.0.4 of December 2019; Groom *et al.* 2016) for the 2,6-diphenylpiperidin-4-one skeleton resulted in 240 hits, which was refined to 44 matches by removing those structures in which the title skeleton substructure was combined with larger molecules. The four most closely related remaining structures based on the pendant arms of the 2,6-diphenylpiperidine-4-one central substructure are 2,6-diphenyl-3-isopropylpiperidin-4-one (ACEZUD; Nilofer Nissa *et al.*, 2001), *t*(3)-pentyl-*r*(2),*c*(6)-diphenylpiperidin-4-one (RUGLOV; Gayathri *et al.*, 2009), 3-(2-chloroethyl)-*r*(2),*c*(6)-diphenylpiperidin-4-one (PEXDII; Rajkumar *et al.*, 2018) and 3-(2-chloroethyl)-*r*(2),*c*(6)-bis(4-fluorophenyl)piperidin-4-one (PEXDOO; Rajkumar *et al.*, 2018). The piperidine ring in the title compound is in a slightly distorted chair conformation, similar to that observed in ACEZUD and PEXDOO but different from the chair conformation seen in RUGLOV and PEXDII. The dihedral angle between the mean planes of pendant phenyl rings is 72.1(1) $^\circ$ in the title compound compared to 76.1(1) $^\circ$ in PEXDOO, whereas it is 59.90(5), 59.1(1) and 63.4(1) $^\circ$ in RUGLOV, PEXDII and ACEZUD, respectively. In all five compounds, various N—H \cdots O and weak C—H \cdots O, C—H \cdots π or C—H \cdots F interactions occur in the crystal.

7. Synthesis and crystallization

A mixture of ammonium acetate (0.100 mol, 7.71 g), 4-fluorobenzaldehyde (0.200 mol, 22.0 ml) and 2-heptanone (0.100 mol, 14.2 ml) in distilled ethanol was heated first to boiling. After cooling, the viscous liquid obtained was

dissolved in ether (200 ml) and shaken with 100 ml concentrated hydrochloric acid. The precipitated hydrochloride of 3-butyl-2,6-bis(4-fluorophenyl)piperidin-4-one was removed by filtration and washed first with a 50 ml mixture of ethanol and ether (1:1) and then with ether to remove most of the coloured impurities. The resulting yellowish base was liberated from an alcoholic solution by adding aqueous ammonia (15 ml) and then diluted with water (200 ml). Then, 1.0 g of the crude sample was dissolved in 100 ml of absolute alcohol, warmed until the sample dissolved, and 2.0 g of animal charcoal added in the resulting solution. The hot solution was filtered and the procedure repeated again. The filtered solution was left for 48 h and colourless prisms of (I) were collected in 75% yield. Analysis for $C_{21}H_{23}F_2NO$ (%): found C 74.24, H 6.16, N 4.03; calculated C 73.45, H 6.75, N 4.08; melting point 381.5 K.



FT-IR (cm^{-1}) (KBr): 3287 ($\nu_{\text{N}-\text{H}}$), 3134, 2929, 2866 ($\nu_{\text{C}-\text{H}}$), 1702 ($\nu_{\text{C=O}}$), 1605, 1508 ($\nu_{\text{C=C}}$), 793 ($\nu_{\text{C}-\text{Cl}}$); ^1H NMR (400 MHz, CDCl_3): δ 7.01–7.45 (*m*, aromatic protons), 4.04 (*d*, H6 proton), 3.68 (*s*, H2 proton), 2.67 (*t*, H5a proton), 2.56 (*dd*, H5e proton), 2.0 (NH proton), 0.95–1.0 $\text{CH}_2(3)$, 1.09–1.15 $\text{CH}_2(2)$, 1.59–1.63 $\text{CH}_2(1)$, 0.74, (*t*, CH_3 alkyl proton); ^{13}C NMR (400 MHz, CDCl_3): δ 129.16, 129.38, 128.18, 128.10, 115.64, 115.56, 115.43, 115.35 (aromatic carbon atoms), 138.52 and 137.64 (*ipso* carbon atoms), 66.33 (C2), 57.50 (C3), 208.7 (C4), 51.63 (C5), 61.08 (C6), 24.30 C18H_2 , 29.71 C19H_2 , 22.75 C20H_2 , 13.81 C21H_3 .

8. Refinement

Crystal data, data collection and structure refinement details are summarized in Table 2. The C-bound H atoms were geometrically placed ($\text{C-H} = 0.93\text{--}0.98 \text{\AA}$) and refined as riding atoms. The N-bound H atom was located in a difference map and its position was fixed. The methyl group was allowed to rotate, but not to tip, to best fit the electron density. The constraint $U_{\text{iso}}(\text{H}) = 1.2U_{\text{eq}}(\text{carrier})$ or $1.5U_{\text{eq}}(\text{methyl carrier})$ was applied in all cases.

Acknowledgements

The authors would like to acknowledge Vellore Institute of Technology, Tamilnadu, India for recording the NMR spectra, the Indian Institute of Technology (IIT), Chennai, Tamilnadu, India for recording the FT-IR and UV-Visible spectra and extend their thanks to the Principal, Dr V. Ramnath, Chairman, Mr R. Sattanathan, and Treasurer, Mr T. Rama-lingam, of Thiruvalluvar Arts and Science College for giving permission to carry out research work in the Chemistry Laboratory.

Funding information

JPJ acknowledges the NSF-MRI program (grant No. CHE1039027) for funds to purchase the X-ray diffractometer.

References

- Arulraj, R., Sivakumar, S., Rajkumar, K., Jasinski, J. P., Kaur, M. & Thiruvalluvar, A. (2019). *J. Chem. Cryst.* **50**, 41–51.
- Arulraj, R., Sivakumar, S., Suresh, S. & Anitha, K. (2020). *Spectrochim. Acta Part A*, **232**, 118166.
- Beddoes, R. L., Dalton, L., Joule, T. A., Mills, O. S., Street, J. D. & Watt, C. I. F. (1986). *J. Chem. Soc. Perkin Trans. 2*, pp. 787.
- Dolomanov, O. V., Bourhis, L. J., Gildea, R. J., Howard, J. A. K. & Puschmann, H. (2009). *J. Appl. Cryst.* **42**, 339–341.
- El-Subbagh, H. I., Abu-Zaid, S. M., Mahran, M. A., Badria, F. A. & Al-Obaid, A. M. (2000). *J. Med. Chem.* **43**, 2915–2921.
- Frisch, M. J., Trucks, G. W., Schlegel, H. B., Scuseria, G. E., Robb, M. A., Cheeseman, J. R., Scalmani, G., Barone, V., Mennucci, B., Petersson, G. A., Nakatsuji, H., Caricato, M., Li, X., Hratchian, H. P., Izmaylov, A. F., Bloino, J., Zheng, G., Sonnenberg, J. L., Hada, M., Ehara, M., Toyota, K., Fukuda, R., Hasegawa, J., Ishida, M., Nakajima, T., Honda, Y., Kitao, O., Nakai, H., Vreven, T., Montgomery, J. A., Jr., Peralta, J. E., Ogliaro, F., Bearpark, M., Heyd, J. J., Brothers, E., Kudin, K. N., Staroverov, V. N., Kobayashi, R., Normand, J., Raghavachari, K., Rendell, A., Burant, J. C., Iyengar, S. S., Tomasi, J., Cossi, M., Rega, N., Millam, J. M., Klene, M., Knox, J. E., Cross, J. B., Bakken, V., Adamo, C., Jaramillo, J., Gomperts, R., Stratmann, R. E., Yazyev, O., Austin, A. J., Cammi, R., Pomelli, C., Ochterski, J. W., Martin, R. L., Morokuma, K., Zakrzewski, V. G., Voth, G. A., Salvador, P., Dannenberg, J. J., Dapprich, S., Daniels, A. D., Farkas, Ö., Foresman, J. B., Ortiz, J. V., Cioslowski, J. & Fox, D. J. (2009). *GAUSSIAN09*. Gaussian Inc., Wallingford, CT, USA.
- Gayathri, P., Jayabharathi, J., Rajarajan, G., Thiruvalluvar, A. & Butcher, R. J. (2009). *Acta Cryst. E65*, o3083.
- Groom, C. R., Bruno, I. J., Lightfoot, M. P. & Ward, S. C. (2016). *Acta Cryst. B72*, 171–179.
- Hehre, W. J., Random, L., Schleyer, P. R. & Pople, J. A. (1986). *Ab initio Molecular Orbital Theory*. New York: Wiley.
- Katritzky, A. R. & Fan, W. J. (1990). *J. Org. Chem.* **55**, 3205–3209.
- McKinnon, J. J., Jayatilaka, D. & Spackman, M. A. (2007). *Chem. Commun.* pp. 3814–3816.
- Mobio, I. G., Soldatenkov, A. T., Federov, V. O., Ageev, E. A., Sergeeva, N. D., Lin, S., Stashenku, E. E., Prostakov, N. S. & Andreeva, E. L. (1989). *Khim. Farm. Zh.* **23**, 421–427.
- Nilofar Nissa, M., Velmurugan, D., Narasimhan, S., Rajagopal, V. & Kim, M.-J. (2001). *Acta Cryst. E57*, o996–o998.

Table 2
Experimental details.

Crystal data	C ₂₁ H ₂₃ F ₂ NO
Chemical formula	
<i>M</i> _r	343.40
Crystal system, space group	Monoclinic, <i>P2</i> ₁ / <i>c</i>
Temperature (K)	173
<i>a</i> , <i>b</i> , <i>c</i> (Å)	5.4945 (3), 25.0707 (13), 12.9811 (9)
β (°)	93.497 (6)
<i>V</i> (Å ³)	1784.83 (18)
<i>Z</i>	4
Radiation type	Cu <i>K</i> α
μ (mm ⁻¹)	0.76
Crystal size (mm)	0.42 × 0.36 × 0.35
Data collection	
Diffractometer	Rigaku Oxford Diffraction Gemini Eos
Absorption correction	Multi-scan (<i>CrysAlis PRO</i> ; Rigaku OD, 2019)
<i>T</i> _{min} , <i>T</i> _{max}	0.803, 1.000
No. of measured, independent and observed [<i>I</i> > 2σ(<i>I</i>)] reflections	6900, 3404, 3045
<i>R</i> _{int}	0.027
(sin θ/λ) _{max} (Å ⁻¹)	0.614
Refinement	
<i>R</i> [$F^2 > 2\sigma(F^2)$], <i>wR</i> (F^2), <i>S</i>	0.045, 0.126, 1.04
No. of reflections	3404
No. of parameters	228
H-atom treatment	H-atom parameters constrained
$\Delta\rho_{\text{max}}$, $\Delta\rho_{\text{min}}$ (e Å ⁻³)	0.26, -0.24

Computer programs: *CrysAlis PRO* (Rigaku OD, 2019), *SHELXT* (Sheldrick, 2015a), *SHELXL* (Sheldrick, 2015b) and *OLEX2* (Dolomanov *et al.*, 2009).

- Rajkumar, K., Sivakumar, S., Arulraj, R., Kaur, M., Jasinski, J. P., Manimekalai, A. & Thiruvalluvar, A. (2018). *Acta Cryst. E74*, 483–486.
- Ramachandran, R., Parthiban, P., Doddi, A., Ramkumar, V. & Kabilan, S. (2007). *Acta Cryst. E63*, o4559.
- Rigaku OD (2019). *CrysAlis PRO*. Rigaku Americas, The Woodlands, Texas, USA.
- Schmidt, J. R. & Polik, W. F. (2007). *WebMO Pro*. WebMO, LLC: Holland. <http://www.webmo.net>
- Sheldrick, G. M. (2015a). *Acta Cryst. A71*, 3–8.
- Sheldrick, G. M. (2015b). *Acta Cryst. C71*, 3–8.
- Spackman, M. A. & Jayatilaka, D. (2009). *CrystEngComm*, **11**, 19–32.
- Turner, M. J., McKinnon, J. J., Wolff, S. K., Grimwood, D. J., Spackman, P. R., Jayatilaka, D. & Spackman, M. A. (2017). *CrystalExplorer17*. The University of Western Australia.

supporting information

Acta Cryst. (2020). E76, 651-655 [https://doi.org/10.1107/S2056989020004636]

Synthesis, crystal structure, DFT calculations and Hirshfeld surface analysis of 3-butyl-2,6-bis(4-fluorophenyl)piperidin-4-one

K. Anitha, S. Sivakumar, R. Arulraj, K. Rajkumar, Manpreet Kaur and Jerry P. Jasinski

Computing details

Data collection: *CrysAlis PRO* (Rigaku OD, 2019); cell refinement: *CrysAlis PRO* (Rigaku OD, 2019); data reduction: *CrysAlis PRO* (Rigaku OD, 2019); program(s) used to solve structure: *ShelXT* (Sheldrick, 2015a); program(s) used to refine structure: *SHELXL* (Sheldrick, 2015b); molecular graphics: *OLEX2* (Dolomanov *et al.*, 2009); software used to prepare material for publication: *OLEX2* (Dolomanov *et al.*, 2009).

3-Butyl-2,6-bis(4-fluorophenyl)piperidin-4-one

Crystal data

$C_{21}H_{23}F_2NO$
 $M_r = 343.40$
Monoclinic, $P2_1/c$
 $a = 5.4945$ (3) Å
 $b = 25.0707$ (13) Å
 $c = 12.9811$ (9) Å
 $\beta = 93.497$ (6)°
 $V = 1784.83$ (18) Å³
 $Z = 4$

$F(000) = 728$
 $D_x = 1.278 \text{ Mg m}^{-3}$
Cu $K\alpha$ radiation, $\lambda = 1.54184$ Å
Cell parameters from 3131 reflections
 $\theta = 0.8\text{--}1.0^\circ$
 $\mu = 0.76 \text{ mm}^{-1}$
 $T = 173$ K
Prism, colourless
0.42 × 0.36 × 0.35 mm

Data collection

Rigaku Oxford Diffraction Gemini Eos diffractometer
Radiation source: fine-focus sealed X-ray tube
Detector resolution: 16.0416 pixels mm⁻¹
 ω scans
Absorption correction: multi-scan (CrysAlisPro; Rigaku OD, 2019)
 $T_{\min} = 0.803$, $T_{\max} = 1.000$

6900 measured reflections
3404 independent reflections
3045 reflections with $I > 2\sigma(I)$
 $R_{\text{int}} = 0.027$
 $\theta_{\max} = 71.3^\circ$, $\theta_{\min} = 3.5^\circ$
 $h = -6 \rightarrow 6$
 $k = -30 \rightarrow 26$
 $l = -9 \rightarrow 15$

Refinement

Refinement on F^2
Least-squares matrix: full
 $R[F^2 > 2\sigma(F^2)] = 0.045$
 $wR(F^2) = 0.126$
 $S = 1.04$
3404 reflections
228 parameters
0 restraints
Primary atom site location: dual
Hydrogen site location: mixed

H-atom parameters constrained
 $w = 1/[\sigma^2(F_o^2) + (0.0664P)^2 + 0.4364P]$
where $P = (F_o^2 + 2F_c^2)/3$
 $(\Delta/\sigma)_{\max} < 0.001$
 $\Delta\rho_{\max} = 0.26 \text{ e } \text{\AA}^{-3}$
 $\Delta\rho_{\min} = -0.24 \text{ e } \text{\AA}^{-3}$
Extinction correction: *SHELXL* (Sheldrick 2015b), $Fc^* = kFc[1 + 0.001xFc^2\lambda^3/\sin(2\theta)]^{-1/4}$
Extinction coefficient: 0.0035 (5)

Special details

Geometry. All esds (except the esd in the dihedral angle between two l.s. planes) are estimated using the full covariance matrix. The cell esds are taken into account individually in the estimation of esds in distances, angles and torsion angles; correlations between esds in cell parameters are only used when they are defined by crystal symmetry. An approximate (isotropic) treatment of cell esds is used for estimating esds involving l.s. planes.

Fractional atomic coordinates and isotropic or equivalent isotropic displacement parameters (\AA^2)

	<i>x</i>	<i>y</i>	<i>z</i>	$U_{\text{iso}}^*/U_{\text{eq}}$
F1	1.1088 (2)	0.45264 (4)	0.91794 (7)	0.0458 (3)
F2	0.2626 (2)	0.04577 (4)	0.65950 (9)	0.0493 (3)
O1	0.9789 (3)	0.28871 (5)	0.32525 (9)	0.0439 (3)
N1	0.8301 (2)	0.26447 (5)	0.61588 (9)	0.0265 (3)
H1	0.859899	0.250816	0.692480	0.032*
C1	1.0000 (3)	0.30675 (6)	0.58925 (11)	0.0267 (3)
H1A	1.163280	0.290264	0.580635	0.032*
C2	0.9099 (3)	0.33248 (6)	0.48525 (11)	0.0278 (3)
H2	0.745757	0.348399	0.494336	0.033*
C3	0.8784 (3)	0.28808 (6)	0.40558 (11)	0.0312 (3)
C4	0.7247 (3)	0.24148 (6)	0.43663 (12)	0.0341 (4)
H4A	0.729221	0.212850	0.384262	0.041*
H4B	0.553231	0.252968	0.440962	0.041*
C5	0.8253 (3)	0.22036 (6)	0.54247 (11)	0.0282 (3)
H5	0.996468	0.207883	0.535604	0.034*
C6	0.6767 (3)	0.17398 (6)	0.57869 (11)	0.0261 (3)
C7	0.7422 (3)	0.12243 (6)	0.55255 (12)	0.0303 (3)
H7	0.883737	0.116949	0.515379	0.036*
C8	0.6046 (3)	0.07877 (6)	0.57975 (13)	0.0344 (4)
H8	0.649053	0.043603	0.561167	0.041*
C9	0.4023 (3)	0.08793 (6)	0.63432 (12)	0.0340 (4)
C10	0.3355 (3)	0.13790 (7)	0.66510 (13)	0.0351 (4)
H10	0.198118	0.142774	0.705110	0.042*
C11	0.4740 (3)	0.18125 (6)	0.63626 (12)	0.0314 (3)
H11	0.429534	0.216223	0.656111	0.038*
C12	1.0247 (3)	0.34625 (6)	0.67737 (11)	0.0265 (3)
C13	1.2301 (3)	0.34492 (6)	0.74451 (13)	0.0350 (4)
H13	1.353733	0.319324	0.734112	0.042*
C14	1.2594 (3)	0.38022 (7)	0.82671 (13)	0.0389 (4)
H14	1.400409	0.378901	0.872784	0.047*
C15	1.0794 (3)	0.41700 (6)	0.83961 (12)	0.0327 (4)
C16	0.8701 (3)	0.41935 (6)	0.77634 (12)	0.0347 (4)
H16	0.747117	0.444956	0.787708	0.042*
C17	0.8432 (3)	0.38332 (6)	0.69539 (12)	0.0312 (3)
H17	0.698502	0.383920	0.651444	0.037*
C18	1.0774 (3)	0.37699 (6)	0.45103 (12)	0.0300 (3)
H18A	1.214626	0.360763	0.416194	0.036*
H18B	1.146589	0.395904	0.513051	0.036*
C19	0.9510 (3)	0.41772 (6)	0.37807 (12)	0.0347 (4)

H19A	1.075666	0.442006	0.352266	0.042*
H19B	0.873544	0.398610	0.317901	0.042*
C20	0.7587 (3)	0.45074 (7)	0.42774 (14)	0.0409 (4)
H20A	0.828276	0.464904	0.494378	0.049*
H20B	0.619586	0.427418	0.442398	0.049*
C21	0.6662 (4)	0.49699 (7)	0.36054 (15)	0.0453 (4)
H21A	0.800002	0.522000	0.351000	0.068*
H21B	0.534931	0.515376	0.394092	0.068*
H21C	0.603886	0.483414	0.293211	0.068*

Atomic displacement parameters (\AA^2)

	U^{11}	U^{22}	U^{33}	U^{12}	U^{13}	U^{23}
F1	0.0703 (7)	0.0351 (5)	0.0321 (5)	-0.0142 (5)	0.0041 (5)	-0.0113 (4)
F2	0.0580 (6)	0.0342 (5)	0.0559 (7)	-0.0176 (5)	0.0041 (5)	0.0125 (5)
O1	0.0700 (8)	0.0380 (6)	0.0248 (6)	-0.0140 (6)	0.0122 (5)	-0.0041 (5)
N1	0.0356 (6)	0.0226 (6)	0.0212 (6)	-0.0038 (5)	0.0004 (5)	0.0010 (4)
C1	0.0301 (7)	0.0244 (7)	0.0255 (7)	-0.0014 (5)	0.0015 (5)	0.0005 (6)
C2	0.0342 (7)	0.0259 (7)	0.0233 (7)	-0.0032 (6)	0.0018 (6)	0.0009 (6)
C3	0.0411 (8)	0.0301 (7)	0.0219 (7)	-0.0048 (6)	-0.0009 (6)	0.0028 (6)
C4	0.0449 (9)	0.0313 (8)	0.0258 (8)	-0.0093 (6)	-0.0010 (6)	-0.0008 (6)
C5	0.0340 (7)	0.0244 (7)	0.0262 (7)	-0.0035 (6)	0.0026 (6)	0.0002 (6)
C6	0.0309 (7)	0.0227 (7)	0.0244 (7)	-0.0013 (5)	-0.0010 (5)	0.0010 (5)
C7	0.0353 (7)	0.0276 (7)	0.0281 (7)	0.0002 (6)	0.0027 (6)	-0.0029 (6)
C8	0.0467 (9)	0.0216 (7)	0.0344 (8)	0.0011 (6)	-0.0031 (7)	-0.0008 (6)
C9	0.0391 (8)	0.0284 (8)	0.0338 (8)	-0.0087 (6)	-0.0040 (6)	0.0093 (6)
C10	0.0335 (7)	0.0358 (8)	0.0365 (9)	-0.0006 (6)	0.0063 (6)	0.0047 (6)
C11	0.0343 (7)	0.0243 (7)	0.0356 (8)	0.0029 (6)	0.0033 (6)	0.0009 (6)
C12	0.0335 (7)	0.0229 (7)	0.0231 (7)	-0.0047 (5)	0.0029 (5)	0.0025 (5)
C13	0.0371 (8)	0.0334 (8)	0.0338 (8)	0.0041 (6)	-0.0029 (6)	-0.0032 (6)
C14	0.0398 (8)	0.0430 (9)	0.0327 (9)	-0.0049 (7)	-0.0075 (7)	-0.0048 (7)
C15	0.0496 (9)	0.0256 (7)	0.0235 (7)	-0.0119 (6)	0.0064 (6)	-0.0038 (6)
C16	0.0430 (8)	0.0301 (8)	0.0316 (8)	0.0033 (6)	0.0074 (6)	-0.0015 (6)
C17	0.0321 (7)	0.0344 (8)	0.0270 (7)	0.0004 (6)	0.0006 (6)	-0.0012 (6)
C18	0.0348 (7)	0.0290 (7)	0.0266 (7)	-0.0063 (6)	0.0045 (6)	0.0004 (6)
C19	0.0460 (9)	0.0294 (8)	0.0293 (8)	-0.0052 (6)	0.0073 (6)	0.0038 (6)
C20	0.0513 (10)	0.0329 (8)	0.0396 (9)	-0.0004 (7)	0.0114 (8)	0.0073 (7)
C21	0.0581 (11)	0.0334 (9)	0.0442 (10)	0.0035 (8)	0.0022 (8)	0.0044 (7)

Geometric parameters (\AA , ^\circ)

F1—C15	1.3559 (17)	C10—H10	0.9500
F2—C9	1.3581 (17)	C10—C11	1.391 (2)
O1—C3	1.2096 (19)	C11—H11	0.9500
N1—H1	1.0549	C12—C13	1.384 (2)
N1—C1	1.4678 (17)	C12—C17	1.393 (2)
N1—C5	1.4590 (18)	C13—H13	0.9500
C1—H1A	1.0000	C13—C14	1.388 (2)

C1—C2	1.5498 (19)	C14—H14	0.9500
C1—C12	1.5128 (19)	C14—C15	1.370 (2)
C2—H2	1.0000	C15—C16	1.373 (2)
C2—C3	1.522 (2)	C16—H16	0.9500
C2—C18	1.5296 (19)	C16—C17	1.387 (2)
C3—C4	1.511 (2)	C17—H17	0.9500
C4—H4A	0.9900	C18—H18A	0.9900
C4—H4B	0.9900	C18—H18B	0.9900
C4—C5	1.543 (2)	C18—C19	1.530 (2)
C5—H5	1.0000	C19—H19A	0.9900
C5—C6	1.5121 (19)	C19—H19B	0.9900
C6—C7	1.389 (2)	C19—C20	1.517 (2)
C6—C11	1.391 (2)	C20—H20A	0.9900
C7—H7	0.9500	C20—H20B	0.9900
C7—C8	1.388 (2)	C20—C21	1.520 (2)
C8—H8	0.9500	C21—H21A	0.9800
C8—C9	1.373 (2)	C21—H21B	0.9800
C9—C10	1.372 (2)	C21—H21C	0.9800
C1—N1—H1	113.1	C6—C11—C10	120.76 (14)
C5—N1—H1	111.4	C6—C11—H11	119.6
C5—N1—C1	112.32 (11)	C10—C11—H11	119.6
N1—C1—H1A	108.4	C13—C12—C1	119.50 (13)
N1—C1—C2	109.37 (11)	C13—C12—C17	118.36 (14)
N1—C1—C12	108.87 (11)	C17—C12—C1	122.12 (13)
C2—C1—H1A	108.4	C12—C13—H13	119.3
C12—C1—H1A	108.4	C12—C13—C14	121.38 (15)
C12—C1—C2	113.29 (11)	C14—C13—H13	119.3
C1—C2—H2	107.8	C13—C14—H14	120.9
C3—C2—C1	107.73 (11)	C15—C14—C13	118.19 (15)
C3—C2—H2	107.8	C15—C14—H14	120.9
C3—C2—C18	112.44 (12)	F1—C15—C14	118.78 (15)
C18—C2—C1	113.01 (12)	F1—C15—C16	118.50 (15)
C18—C2—H2	107.8	C14—C15—C16	122.72 (14)
O1—C3—C2	122.51 (14)	C15—C16—H16	120.9
O1—C3—C4	122.15 (14)	C15—C16—C17	118.15 (15)
C4—C3—C2	115.25 (12)	C17—C16—H16	120.9
C3—C4—H4A	109.9	C12—C17—H17	119.4
C3—C4—H4B	109.9	C16—C17—C12	121.17 (14)
C3—C4—C5	109.09 (12)	C16—C17—H17	119.4
H4A—C4—H4B	108.3	C2—C18—H18A	108.7
C5—C4—H4A	109.9	C2—C18—H18B	108.7
C5—C4—H4B	109.9	C2—C18—C19	114.09 (12)
N1—C5—C4	108.21 (12)	H18A—C18—H18B	107.6
N1—C5—H5	108.4	C19—C18—H18A	108.7
N1—C5—C6	111.60 (12)	C19—C18—H18B	108.7
C4—C5—H5	108.4	C18—C19—H19A	108.8
C6—C5—C4	111.70 (12)	C18—C19—H19B	108.8

C6—C5—H5	108.4	H19A—C19—H19B	107.7
C7—C6—C5	119.12 (13)	C20—C19—C18	113.74 (13)
C7—C6—C11	118.74 (14)	C20—C19—H19A	108.8
C11—C6—C5	122.13 (13)	C20—C19—H19B	108.8
C6—C7—H7	119.4	C19—C20—H20A	109.0
C8—C7—C6	121.23 (14)	C19—C20—H20B	109.0
C8—C7—H7	119.4	C19—C20—C21	112.94 (14)
C7—C8—H8	121.0	H20A—C20—H20B	107.8
C9—C8—C7	118.03 (14)	C21—C20—H20A	109.0
C9—C8—H8	121.0	C21—C20—H20B	109.0
F2—C9—C8	118.78 (14)	C20—C21—H21A	109.5
F2—C9—C10	118.38 (15)	C20—C21—H21B	109.5
C10—C9—C8	122.84 (14)	C20—C21—H21C	109.5
C9—C10—H10	120.8	H21A—C21—H21B	109.5
C9—C10—C11	118.34 (15)	H21A—C21—H21C	109.5
C11—C10—H10	120.8	H21B—C21—H21C	109.5
F1—C15—C16—C17	178.97 (13)	C4—C5—C6—C11	-88.66 (17)
F2—C9—C10—C11	-177.84 (14)	C5—N1—C1—C2	64.80 (15)
O1—C3—C4—C5	123.39 (17)	C5—N1—C1—C12	-170.93 (11)
N1—C1—C2—C3	-54.89 (15)	C5—C6—C7—C8	-176.87 (13)
N1—C1—C2—C18	-179.73 (12)	C5—C6—C11—C10	177.54 (14)
N1—C1—C12—C13	102.72 (15)	C6—C7—C8—C9	-0.6 (2)
N1—C1—C12—C17	-75.42 (16)	C7—C6—C11—C10	-1.5 (2)
N1—C5—C6—C7	-148.28 (13)	C7—C8—C9—F2	178.51 (13)
N1—C5—C6—C11	32.63 (19)	C7—C8—C9—C10	-1.8 (2)
C1—N1—C5—C4	-64.54 (15)	C8—C9—C10—C11	2.5 (2)
C1—N1—C5—C6	172.17 (11)	C9—C10—C11—C6	-0.7 (2)
C1—C2—C3—O1	-124.44 (16)	C11—C6—C7—C8	2.2 (2)
C1—C2—C3—C4	52.03 (17)	C12—C1—C2—C3	-176.53 (12)
C1—C2—C18—C19	-155.74 (13)	C12—C1—C2—C18	58.63 (16)
C1—C12—C13—C14	-179.62 (14)	C12—C13—C14—C15	-0.5 (3)
C1—C12—C17—C16	-179.67 (14)	C13—C12—C17—C16	2.2 (2)
C2—C1—C12—C13	-135.36 (14)	C13—C14—C15—F1	-178.24 (14)
C2—C1—C12—C17	46.50 (18)	C13—C14—C15—C16	1.7 (2)
C2—C3—C4—C5	-53.09 (18)	C14—C15—C16—C17	-1.0 (2)
C2—C18—C19—C20	66.24 (18)	C15—C16—C17—C12	-1.0 (2)
C3—C2—C18—C19	82.03 (16)	C17—C12—C13—C14	-1.4 (2)
C3—C4—C5—N1	55.98 (16)	C18—C2—C3—O1	0.7 (2)
C3—C4—C5—C6	179.22 (13)	C18—C2—C3—C4	177.20 (13)
C4—C5—C6—C7	90.43 (16)	C18—C19—C20—C21	170.21 (14)

Hydrogen-bond geometry (Å, °)

Cg3 is the centroid of the C12—C17 ring.

D—H···A	D—H	H···A	D···A	D—H···A
N1—H1···O1 ⁱ	1.05	2.06	3.0921 (16)	165
C7—H7···F1 ⁱⁱ	0.95	2.52	3.3291 (18)	143

C10—H10···O1 ⁱⁱⁱ	0.95	2.66	3.470 (2)	144
C16—H16···F2 ^{iv}	0.95	2.62	3.3680 (18)	136
C21—H21C···F2 ⁱⁱ	0.98	2.58	3.489 (2)	154
C21—H21A···Cg3 ^v	0.98	2.95	3.793 (2)	145

Symmetry codes: (i) $x, -y+1/2, z+1/2$; (ii) $x, -y+1/2, z-1/2$; (iii) $x-1, -y+1/2, z+1/2$; (iv) $-x+1, y+1/2, -z+3/2$; (v) $-x+2, -y+1, -z+1$.